TL and ESR of quartz from the astrobleme of Aorounga (Sahara of Chad)

Didier Miallier, S. Sanzelle, C. Falgueres, Jean Fain, Thierry Pilleyre, P.M. Vincent

Pergamon

Quaternary Science Reviews (Quaternary Geochronology), Vol. 16, pp. 265–274, 1997.

0277–3791/97 $32.00

PII: S0277–3791(96)00086–8

TL AND ESR OF QUARTZ FROM THE ASTROBLEME OF AOROUNGA (SAHARA OF CHAD)

D. MIALLIER,* S. SANZELLE,* C. FALGUÈRES,† J. FAÏN,* TH. PILLEYRE* and P.M. VINCENT‡

*Laboratoire de Physique Corpusculaire, IN2P3-CNRS, Université Blaise Pascal, 63177 Aubière Cedex, France

†Laboratoire de Préhistoire du Muséum National d'Histoire Naturelle (MNHN), UMR 9948 du CNRS 1, rue R. Panhard, 75013 Paris, France

‡Centre de Recherche Volcanologique, Université Blaise Pascal, 5, rue Kessler, 63000 Clermont-Ferrand, France

Abstract — The present work was intended to evaluate the time that elapsed since the meteorite fall that produced the giant astrobleme of Aorounga (Sahara of Chad). For this purpose the TL and ESR dating techniques using the additive dose method were applied to quartz grains extracted from an impactite and from a sandstone shocked and baked during the impact. The ESR Al centre was measured and resulted in an age of about 800 ka. The red TL and the blue TL showed unusual TL features: the additive dose response curves were marked by an initial saturated part followed by a second rise at around +0.5 kGy; the peaks showed erratic temperature shifts with dose; fading was observed for high temperature peaks. By comparison with previous work using samples baked by lava flows more than 1 Ma ago and presenting some of those features, it was assumed that the minimum age of the astrobleme was of the same order of magnitude. This is in agreement with other observations. A preliminary explanation for those ageing features is proposed. It is suspected that radiation induced traps contribute to the TL of the studied quartz grains. Most probably the 'malign-behaviour' of the quartz grains is also connected with shock effects. © 1997 Elsevier Science Ltd

INTRODUCTION

The astrobleme (meteorite impact crater) of Aorounga is situated in the desert plain of Borkou, 100 km SE of the Emi Koussi volcanic massif, Northern Chad. It lies within Palaeozoic sandstones belonging to the SW part of the Kufra sedimentary basin which, at this location, has a thickness of around 2000 m. Although the 13 km in diameter circular structure has been known for a long time, only recently has it been recognised as originating from a giant meteorite impact: this was mainly on the basis of the presence of shocked quartz (Becq-Giraudon *et al.*, 1992). The main structural features of the astrobleme are so remarkably well preserved that Becq-Giraudon *et al.* assumed a Late Quaternary age between 12,000 and 3,500 BP for the meteorite impact.

The general structural organisation of the astrobleme was studied by Vincent *et al.* (1994). The inner zone of the astrobleme is an uplifted block of Devonian sandstones. It is unconformably covered with a blanket of fluidized impactite flow, in the manner of a pyroclastic flow (Vincent *et al.*, 1994). The underlying sandstones are baked, and reddened by oxidation, attesting to the high temperature of the impactite.

Samples were collected at the ground surface in order to estimate the age of the impact by use of radiochronological methods (because access to the site is difficult, no powered drilling nor excavation could be performed). The present paper gives the results obtained using thermoluminescence (TL) and electron spin resonance (ESR) dating techniques. TL dating has already been successfully applied to a meteorite crater in Arizona by Sutton (1985a, b), giving a TL age of 49±3 ka for the Meteor Crater.

Sample OR9 is a dark-red sandstone from the central plateau. Sample AO5 is an impactite resting on the inner crown: it looks like a fine-grained quartzite, with small rounded detrital quartz grains. In thin section, both samples seem to have been affected by shock metamorphism, with several sets of planar deformation features (PDFs). Such features are among the criteria that characterize class 3 of Kieffer Petrographic Shock Classification (Kieffer, 1971, cited in Sutton, 1985a).

The samples contained more than 92% of SiO_2 (Table 1), the majority of which was in the form of

TABLE 1. Radionuclide and major element data for the samples OR9 (sandstone), AO5 (impactite) and for the quartz extracted from OR9. ^{238}U, ^{232}Th and ^{40}K contents were obtained using low-background gamma spectrometry. External alpha activity was evaluated using thick source alpha counting (TSAC); for comparison, theoretical alpha counting derived from U and Th contents is also given in brackets. Major elements were analysed by F. Cantagrel (Centre de Recherches Volcanologiques, Université Blaise Pascal, Clermont-Ferrand) using ICP

Sample ref.	[Th] (ppm)	[U] (ppm)	Alpha counts ($\alpha cm^{-2}d^{-1}$)	[K_2O] (%)	[SiO_2] (%)	[Al_2O_3] (%)	[Fe_2O_3] (%)	[CaO] (%)
OR9	4.15±0.1	0.58±0.06	22±0.2 (21±2)	0.027±0.013	92.7	2.73	1.79	0.16
AO5	0.52±0.04	0.49±0.06	9.35±0.90 (8±0.8)	0.031±0.013	>95	0.11	0.37	0.09
OR9:quartz	0.66±0.03	0.18±0.05	-	0.01±0.01				

quartz grains. Pure quartz grains were obtained by standard methods, including crushing the samples, HF etching and density separation. No anomaly was observed in the quartz XRD patterns (Y. Blanc, Univ. Blaise Pascal, *pers. commun.*). The proportion by mass of heavy minerals removed using heavy liquids was very little, between 0.06 and 0.3%; this fraction was dominated by zircon grains.

For both samples two sets of sieved quartz grains were selected. The first one was divided in aliquots of around 200 mg, which were given additive gamma radiation doses using a ^{137}Cs gamma source, and the second one was annealed at 380°C in air for one night prior to irradiation. Those two sets of prepared samples were used for TL and for ESR measurements ('additive' measurements using the first set and 'regenerated' using the second one).

TL MEASUREMENTS

Preliminary Measurements

As the first step, an attempt was made to evaluate the palaeodose using the routine additive dose technique.

The red TL was measured through a long-pass short-cut filter (RG610 Schott). The shape of the glow curves was not qualitatively different from the usual red TL signal from quartz (Miallier *et al.*, 1991; Fig. 1). The 350–370°C peak shifted towards low temperatures with increased dose as usual for AO5 but for OR9—measured in a larger dose range—the curve showing the peak shift with dose was sinuous (Fig. 2). For both samples (AO5 and OR9) the additive dose response curve (ADRC) exhibited a shape characterised by a very weak initial growth followed by a 'second rise' and terminated by saturation appearing at around +10 kGy (Fig. 3). The regenerated dose response curve (RDRC) was sinuous: its initial rise, roughly saturating exponential, was also followed by a second rise beginning at around 500 Gy and terminated by saturation.

The blue TL was measured through a red-cutting band-pass filter BG12 Leitz. The natural TL (NTL) for sample OR9 had two peaks (Fig. 4) centred at about 485°C (peak A) and 347°C (peak B). The growth of peak B with added dose is very similar to the growth of the red TL, either for ADRC or RDRC (Fig. 5). The natural peak A seems to be saturated up to around +2 kGy and apparently rises above this dose; but this second rise probably only originated from the high temperature side of peak B, which has by then become very important. For the additive glow curves, peak B appeared at the same temperature, 347°C, up to around +400 Gy and then shifted towards high temperatures with added dose; for the regenerated glow curves the peak continuously shifted towards high temperatures (Fig. 6). For sample AO5 a broad peak centred at about 350°C was observed for the natural signal and for the lower added doses (Fig. 7, peak B′). However, for added doses higher than about +400 Gy, the TL in this region was dominated by a peak B rising at around 370°C; the transition between B′ and B is clear on the curves giving the peak temperature vs dose (Fig. 8). The dose response curves, either plotted for peak height or for a given temperature, still behaved the same as the red TL and peak B for OR9. The ADRC consisted of an initial part which was nearly saturated (up to about +500 Gy), a second rise and a final saturated level commencing around +10 kGy. The RDRC had an initial saturating tendency, a second rise and a saturation.

It was not possible to evaluate palaeodoses using a simple function for extrapolating the red and blue

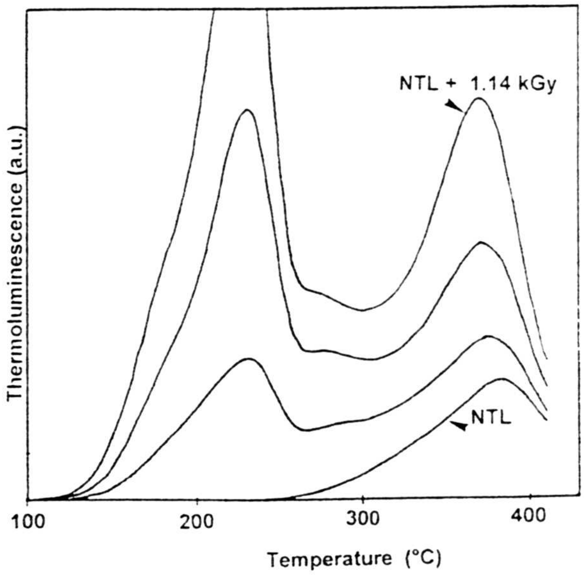

FIG. 1. Additive glow curves for sample AO5. Red filter RG 610 Schott, 5 K/s heating rate, blackbody background subtracted.

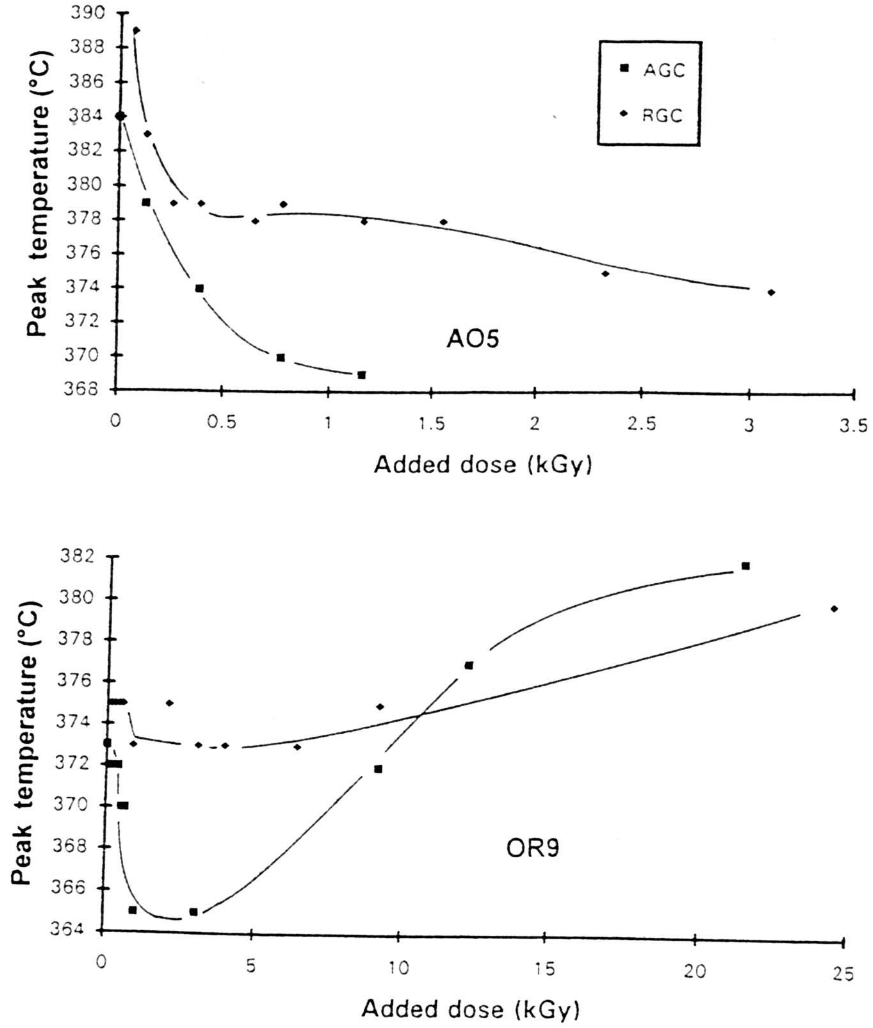

FIG. 2. Plot of the temperature of the red peak vs added dose for quartz samples OR9 and AO5. AGC, additive glow curves; RGC, regenerated glow curves. The lines were drawn free hand for better clarity; they do not pretend to fit the data. Uncertainty on the temperatures is around 2 C.

ADRCs. Also, for all the measured peaks, the difference between the shapes of the RDRCs and the ADRCs precluded the use of a slide technique.

Further Experiments

Fading was tested by comparing the signals for a freshly irradiated sample (+1 kGy) and a sample irradiated 22 months before (an intermediary measurement was made after 3 months). The results (Table 2) indicate that all blue peaks faded, but the amount of signal loss for peak B was the same for 3 months and 22 months (within error limits), thus suggesting a diminution of the fading rate with time as usually observed. On the contrary, the red TL has shown a *recuperation* tendency, which had already been previously observed for quartz, but to a lesser extent (Miallier *et al.*, 1991): the TL of the freshly irradiated sample was lower by around 10% than the TL of the sample irradiated 22 months before.

TABLE 2. Results of fading tests. Columns 2 and 3 give the ratios of the TL intensities for samples irradiated at the same dose: (sample freshly irradiated)/(sample irradiated 3 or 22 months before)

Peak	Intensity variation (3 months)	Intensity variation (22 months)
Red 360 C		0.9±0.06
Red 220 C		0.85±0.07
Blue 130 C		≃70
Blue 220 C		1.15±0.10
Blue 350 C(B)	1.05±0.05	1.05±0.045
Blue 485 C(A)		1.07±0.045

The effect of alpha particles was tested using annealed quartz grains from OR9 (grain size 63–100 μm). The source was made of ^{241}Am delivering 4.5 MeV alpha particles with a flux of 8.4×10^5 αcm^{-2}s^{-1} at the sample level. The blue glow curves have shown peaks A and B rising at constant temperatures, 485 and 370 C, respectively. The RDRC was linear for B and saturating for A (Fig. 9).

ESR

ESR was performed (at MNHN, Paris) using a spectrometer Varian E109 using a microwave power of 5 mW and frequency of 9 GHz (X band). Measurements

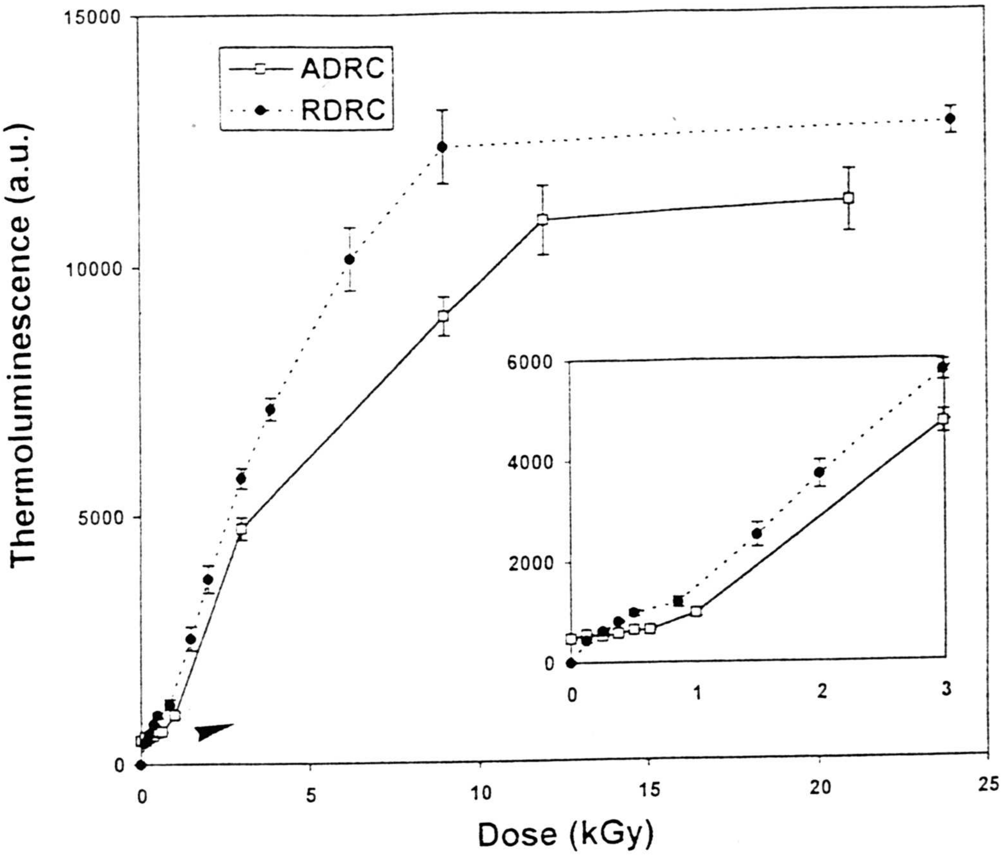

FIG. 3. Dose, response curves plotted for height for the red TL of sample AO5. ADRC, additive curve; RDRC, regenerated curve. Every dose point was averaged over 7–9 curves, measured using 9 mg aliquots of quartz grains. Error bars correspond to one standard deviation. The first part of the curves was enhanced (bottom right). The lines are drawn free hand, they do not pretend to fit the data.

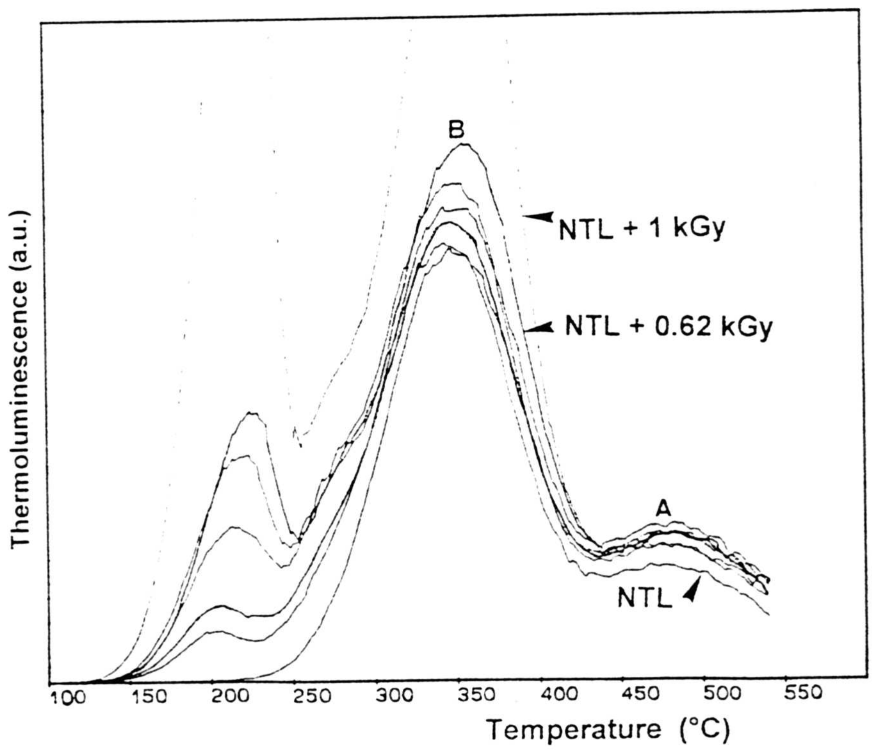

FIG. 4. Additive glow curves for sample OR9, using a blue filter BG12 Leitz; 5 K/s heating rate.

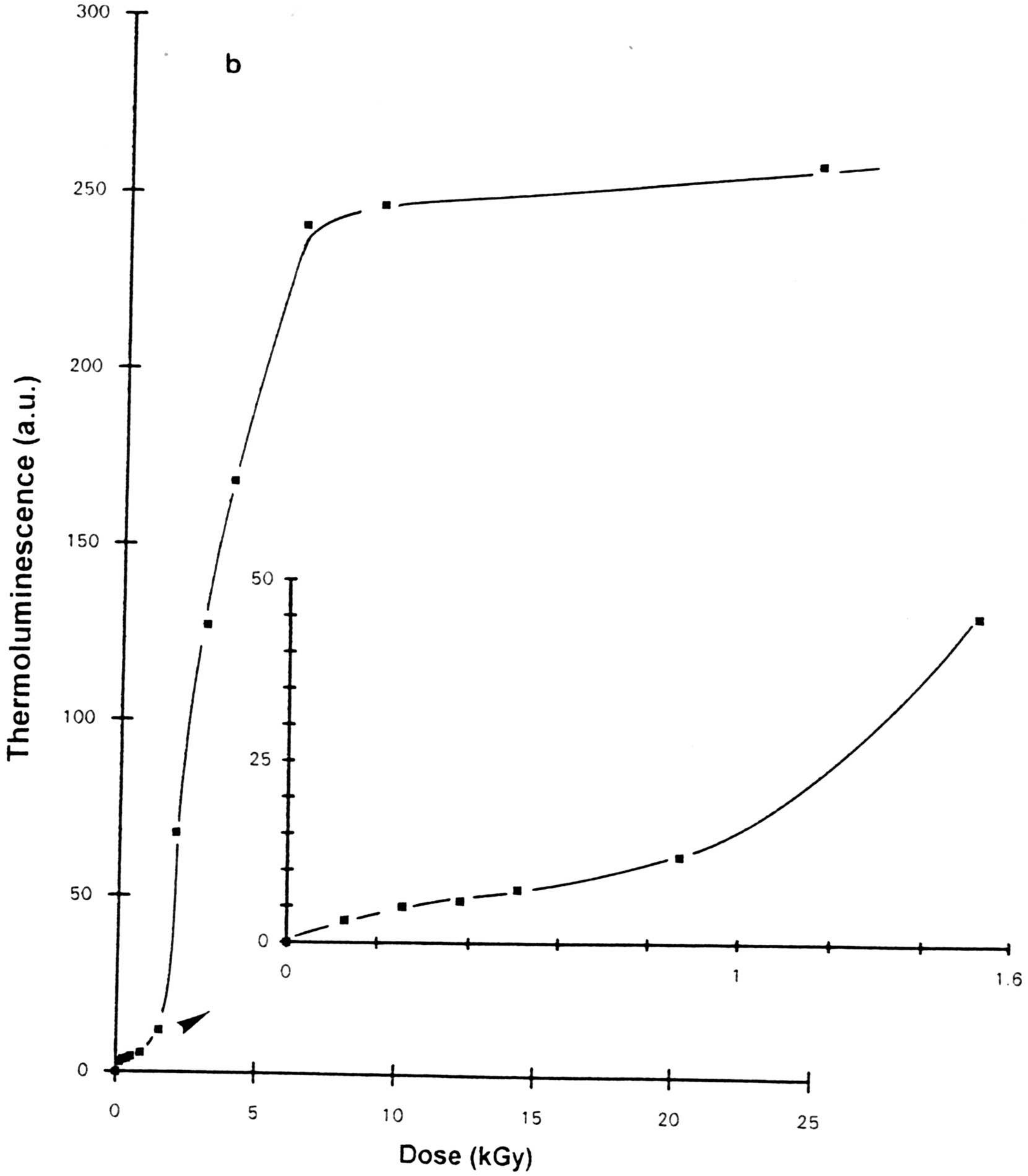

FIG. 5. Dose response curves for sample OR9 plotted for height of the blue peaks (A and B as in Fig. 4). a. additive dose response curves for peaks A and B; b. regenerated dose response curve (peak B). Error bars, not reported, are around 5% of the intensities.

were made at 93 K using 200 mg aliquots of quartz grains.

ESR measurements for sample OR9 gave an unsaturated Al centre (Fig. 10), presenting roughly similar shapes for ADRC and RDRC (Fig. 11). A lower limit of around 400–500 Gy for the palaeodose was estimated using a slide technique. A strong and steady E′ centre was also observed at room temperature. ESR spectra for AO5 were too poorly defined for accurate measurement.

Dosimetry

The internal (i.e. from alpha and beta particles) annual dose rate was estimated using thick source alpha counting (TSAC) and low-background gamma spectrometry (see Table 1). The external gamma dose rate was derived from the analysis of the samples because no measurements could be made *in situ*. The calculated cosmic contribution, around 240 mGy/ka (using data from Prescott and Stephan, 1982, and Prescott and Hutton, 1988) attained between one-third and one-half of the total dose.

Large uncertainties must be considered for gamma and cosmic dose rates; they are due to ignorance of both the erosion rate and variations of the cosmic yield in the past (Prescott and Hutton, 1994). On the ground surface the gamma dose rate cannot be calculated using the infinite matrix assumptions and the soft component of the cosmic radiation is not negligible. On the other hand, between 0 and around 100 g/cm^2 the sum of those two components

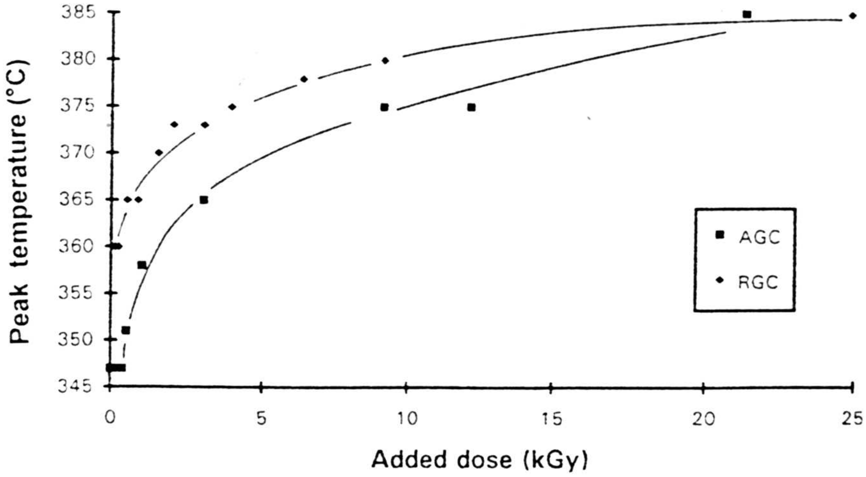

FIG. 6. Plot of the apparent temperature of blue peak B vs dose for sample OR9. AGC, additive glow curves; RGC, regenerated glow curves.

remains approximately constant because the gamma dose becomes higher and the cosmic dose lower when the thickness of rock above the samples is increased. This sum (~460 mGy/ka) was tentatively added to the internal dose to obtain an estimate of the total annual dose D. D was evaluated at 760±80 mGy/ka for OR9 and 510±50 mGy/ka for AO5 (this is for 200–315 μm quartz grains): the relative efficiency for alpha particles coming from inside the quartz grains was assumed to be 10%.

DISCUSSION

From the TL data presented here, the red and blue peaks are clearly disconnected, as are the two blue peaks, A and B. Let us for example compare the growth of those last peaks under alpha radiation: a linear growth was observed for B (as usual for alpha induced TL), whereas a saturating growth for A suggests a complex phenomenon including diffusion of defects between alpha tracks (at 2×10^{10} α/cm^2, corresponding to around 3 kGy, the mean distance between the tracks is around 75 nm). However, the peculiar shapes of the dose response curves are common to the TL peaks studied in the present work. For those shapes, only qualitative crude explanations can be proposed in this preliminary approach.

TL ADRCs, characterised by a very weak initial growth followed by a second rise, have already been observed for quartz samples that were baked by two lava flows previously dated at 2 and 14 Ma by means of the K-Ar technique (Pilleyre, 1991; Pilleyre *et al.*, 1992). And for the samples studied by Pilleyre, as in the present case, the RDRCs were different in shape from the ADRCs (actually the RDRCs obtained by Pilleyre did not show any intermediary saturating portion like in the present case and were monotonic up to the final saturation). Therefore, one can provisionally make the assumption that this kind of dose response curve is connected with 'very old' samples.

A possible cause of the initial 'plateau' may be seen in the presence of competing short-lived traps (not necessarily TL traps) that are to be filled and saturated before the TL traps begin to be significantly filled. Such traps must supposedly be radiation induced, at a low rate, and erased

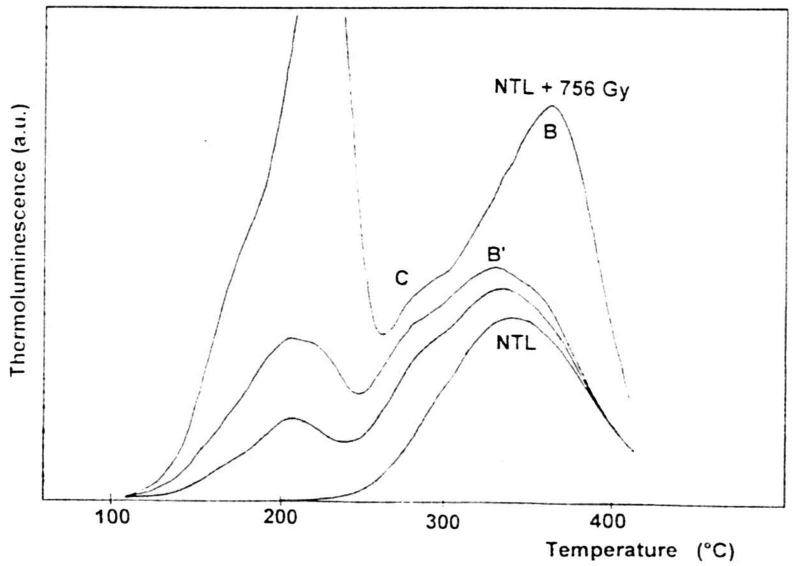

FIG. 7. Additive glow curves for sample AO5. (The 485°C peak, not shown on this figure, is also present as for sample OR9.)

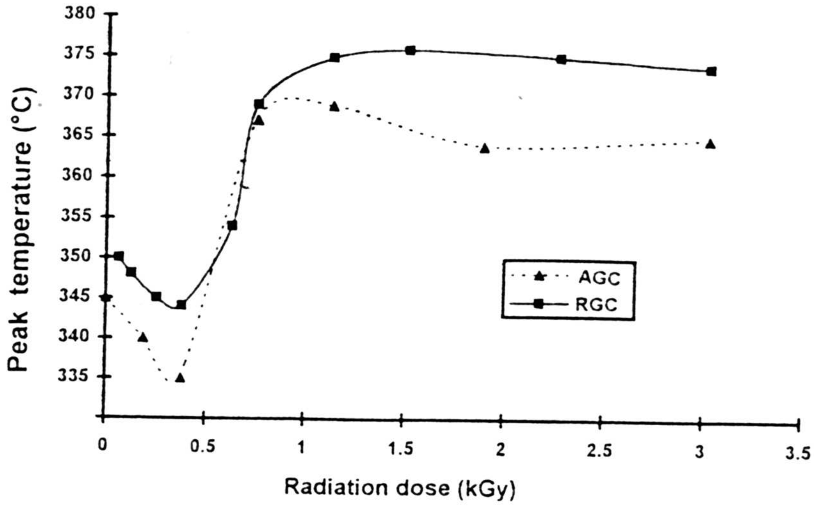

FIG. 8. Plot of the apparent temperature of the blue peak B/B′ as in Fig. 7.

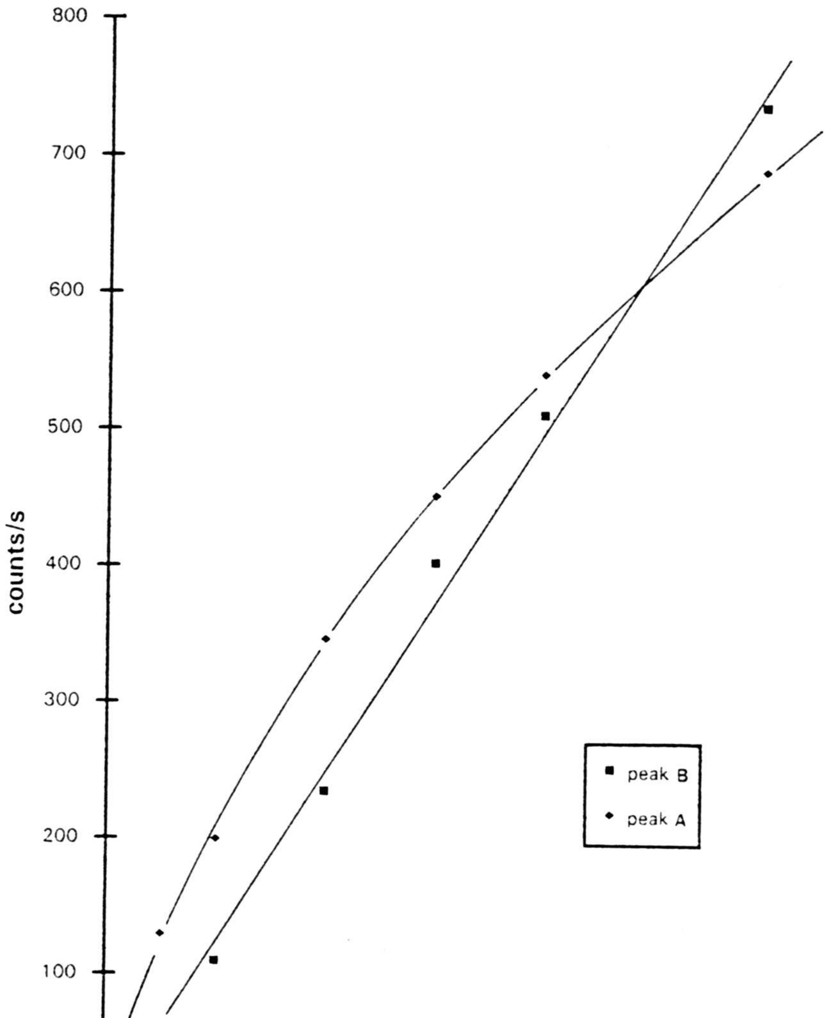

FIG. 9. Regenerated dose response curves for alpha irradiated quartz grains from sample OR9. Grain size 63–100 μm.

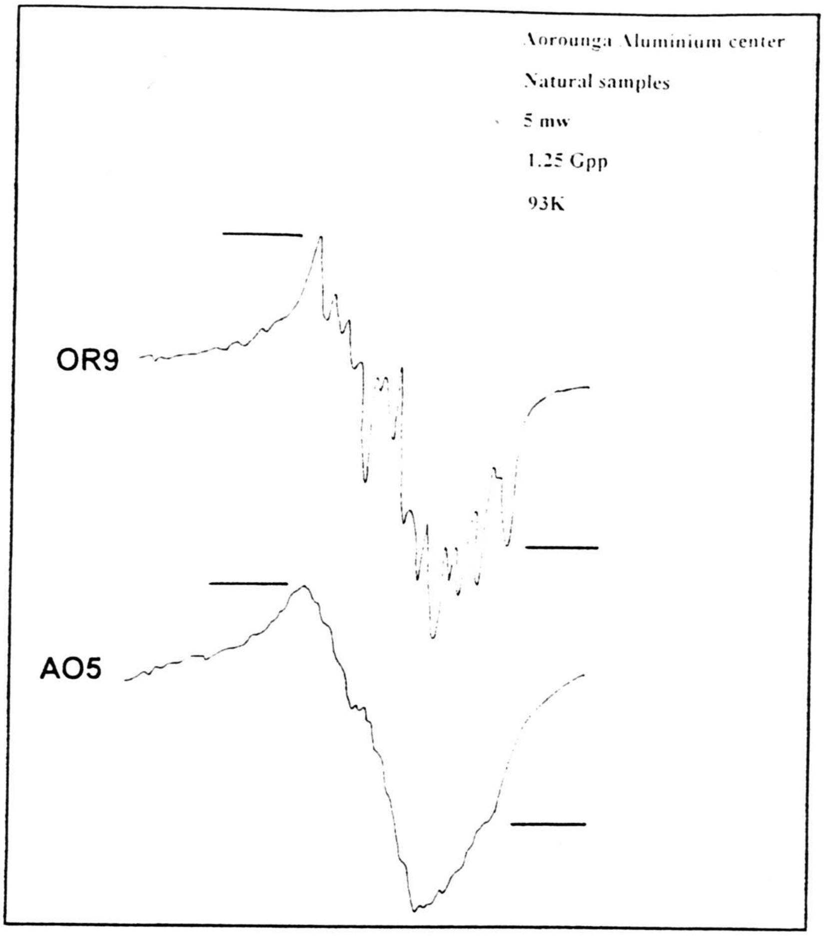

FIG. 10. ESR spectra measured using 200 mg of quartz grains. The bars indicate where the signal was measured for OR9.

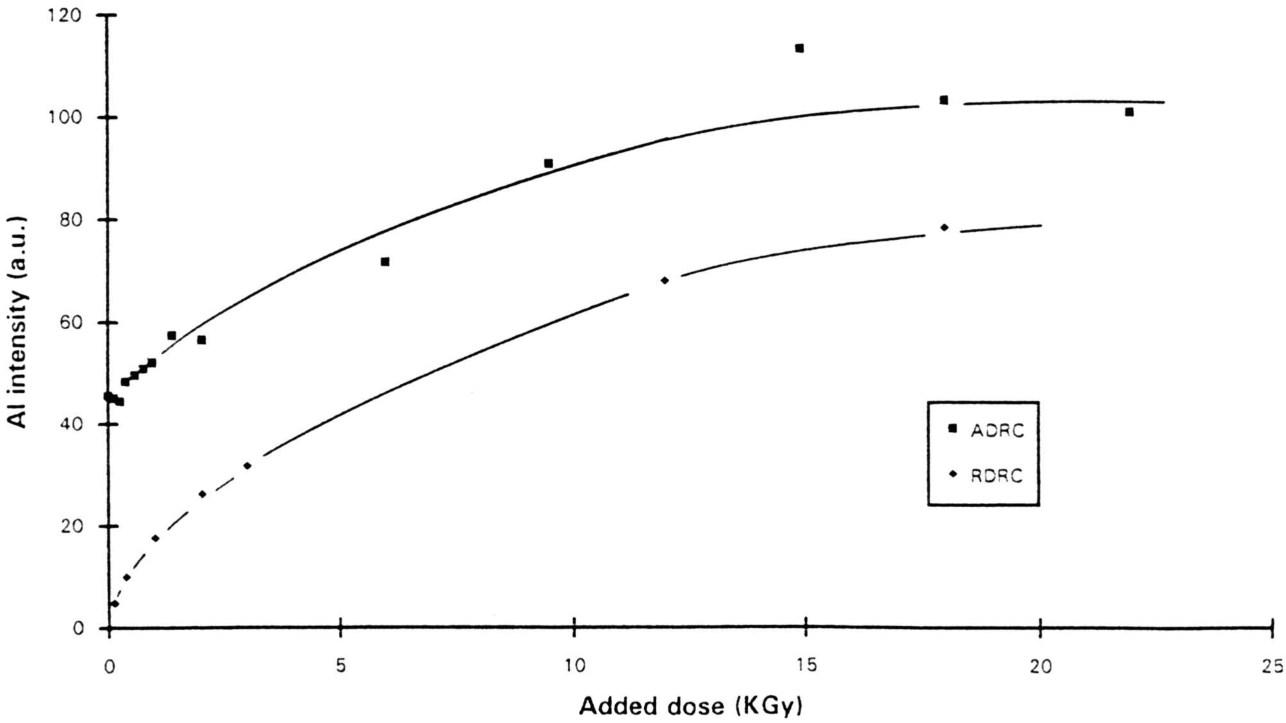

FIG. 11. Dose response curves for the Al ESR centre for sample OR9. The lines are drawn free hand; they do not fit the data. Errors are estimated in the range 5–10% of the signal intensity.

by heat, thus explaining why the phenomenon is visible only with very old samples and weak or absent for the RDRC. This is supported by the observation that the present quartz samples are susceptible to the production of radiation induced traps, as will be seen later. Note that TL measurements were made using quartz grains annealed at 580°C, instead of 380°C, in order to verify if the RDRC still had the same shape. As a result, the glow curves were significantly different: peak A no longer existed and peak B was overlapped by a prominent peak centred at 300°C (which RDRC looked like the preceding ones).

With this in mind, the following experiment was made. Aliquots of the natural quartz OR9 (100–200 μm) were additively irradiated in steps of 370 Gy. Between every irradiation of 370 Gy, all the aliquots were annealed together at about 200°C for 0.5 h. This was intended to empty the shallow traps and simulate qualitatively the irradiation in nature, where those shallow traps (possibly including the competing traps) are always empty. The corresponding additive dose response curve was plotted after TL measurements. It showed a shape similar to the one for the sample irradiated in the usual way, i.e. with a very weak initial growth. But this initial part was extended up to around +1.5 kGy, instead of around +0.5 kGy as found previously. Thus, it seems that the effect was accentuated: this is in favour of the proposed model.

On the other hand, the sudden appearance of peak B also accounts for the second rise, at least for the blue TL of AO5, although this was not the case for the samples studied by Pilleyre (1991), where the shape of the glow curves remained remarkably the same whatever the dose. This raises the question as to whether there are two different mechanisms underlying supralinearity in the ADRC or there is a single complex one.

The blue peak B has characteristic features very similar to those shown by the high temperature peaks of lithium fluoride, LiF, that are supposedly connected with radiation induced traps (Charalambous and Petridou, 1976; Montret, 1980).

- Under gamma irradiation the peak appears suddenly above a certain dose threshold (around +0.5 kGy) and has supralinear growth.
- Under alpha irradiation, the peak appears at lower doses than under gamma irradiation (lowest alpha dose applied in the present case, ~0.22 kGy); it shows a linear growth. The efficiency of alpha radiation compared to gamma radiation seems to be very low, around 2–3%.

In the alpha tracks, the density of defects is very high: thus the density threshold necessary for the appearance of the new traps is attained in every track and hence peak B can exist whatever the total dose. Its growth is linear because it will depend on the number of tracks only; and there is no diffusion of defects or charges between the tracks, at least below the maximum density of tracks studied here, which corresponds to a mean distance between the tracks of about 75 nm.

The traps involved are created and filled under irradiation, and this explains supralinearity; they are erased by heating, and this explains why the same phenomenon is visible for additive glow curves and regenerated glow curves.

Peak B is not present on the natural blue signal, for A05 it is clear, for OR9 the appearance of the peak is announced by the sudden shift in temperature, around +400 Gy. This can be interpreted in different ways:

(1) the trapped charges, or alternatively the traps themselves, are affected by fading,
(2) the palaeodose is lower than the threshold above which the peak rises (if it was the case, this could afford an indication on the order of magnitude of the palaeodose), or
(3) the peak can appear under high dose rates, as under laboratory irradiation but not under low dose rates as in nature (dose rate effect).

Actually, fading (1) was observed, whereas it is usually not measurable for the quartz TL above about 200°C (on the glow curves). The question remains whether it is limited or continuously acting and able to prevent the appearance of peak B under natural conditions. Proposition (2) is not realistic; especially, it would correspond to a very low palaeodose, because for ADRC and RDRC the peak rises nearly at the same added dose.

One can wonder whether those particular TL features for quartz are due to ageing effects or shock metamorphism. We would say both. The similarity between the shape of the dose response curves of the present samples and very old samples previously examined has been outlined. On the other hand, other features like anomalous fading, sudden rise of peak B and peak shift towards high temperatures are peculiar. It is likely that the enormous stress sustained by the grains during the impact has induced a high density of structural defects. Although Sutton (1985a) did not mention similar observations (i.e. ill-behaved quartz), he demonstrated that the sensitivity of quartz was shock dependent. This corroborated experiments reported by David *et al.* (1979) on the variations of the TL sensitivity of quartz submitted to stress. If shock effects do control some TL characteristics in the present case, the observed differences between the two samples can be explained by different shock grades.

Age Estimation

Initial zeroing can be questioned. In fact Sutton (1985a) verified that zeroing was complete for shock class 3. It is not easy to know the role of stress itself in the zeroing process; however, heating only would have been enough since 200°C for half a day is enough to anneal the TL of quartz. In the present case, not only did the temperature during the impact probably go above thousands of degrees, but cooling would have lasted for months. In the case of the Meteor Crater, the size of which is 10 times smaller, the cooling duration was estimated to be around 115 days (Sutton, 1985a). The oxidisation of iron in sample OR9, which required a high temperature, is a further indication of initial resetting by heat.

An estimation of the age can derive from various approaches.

By analogy with the samples older than 1 Ma, which have shown the same peculiar additive dose response curves, we can suppose that the age, in the present case, is also older than about 1 Ma. The TL ADRCs cannot be simply extrapolated for getting the palaeodose; however, using a free-hand method and the lower part of the curves one can estimate palaeodoses higher than about 500 Gy, which will give more than 800 ka for the age.

For ESR the palaeodose estimated from the Al centre results in an age of around 800 ka. Since the life time of this centre is not precisely known (especially for the present unusual quartz sample) it is more secure to consider 800 ka as a minimum age. The presence of the E' centre, which usually takes a very long time, more than several hundreds of thousand years, for recovering (Falguères *et al.*, 1994), is a further indication of the order of magnitude of the age.

Those indications of a minimum age in the range 0.5–1 Ma were confirmed by measurements of the cosmogenic nuclides ^{10}Be and ^{26}Al, which resulted in a minimum age of around 0.5 Ma (Bourles *et al.*, 1995).

CONCLUSION

The quartz grains from the astrobleme of Aorounga have shown unusual TL features, which preclude a real datation. Those features are attributed to both shock and ageing effects.

The meteorite fall that produced the astrobleme of Aorounga did not take place during the Holocene period as previously assumed by Becq-Giraudon *et al.* (1992). Instead is it older than at least 500 ka, but because so many remains unknown, a true age significantly older than this limit cannot be excluded.

ACKNOWLEDGEMENTS

Acknowledgements to Y. Blanc, Centre de Recherche Volcanologique, Université Blaise Pascal, Clermont-Ferrand, for XRD analysis.

REFERENCES

Becq-Giraudon, J.F., Rouzeau, O., Goachet, E. and Solages, S. (1992) Impact hyper-véloce d'une météorite géante à l'origine de la dépression circulaire d'Aorounga au Tchad (Afrique). *Comptes Rendus de l'Académie des Sciences, Paris* **315**, 83–88.

Bourles, D.L., Brown, E.T., Raisbeck, G.M., Yiou, F. and Vincent P. (1995) Exposure age dating of the Aorounga (Sahara) impact crater by *in-situ*-produced ^{10}Be and ^{26}Al. *E.U.G8 Conference Abstract*, Strasbourg, France, 9–13 April 1995.

Charalambous, S. and Petridou, Ch. (1976) The thermoluminescence behaviour of LiF(TLD-100) for doses up to 10 MRad. *Nuclear Instruments and Methods* **137**, 441–444.

David, M., Sunta, C.M. and Ganguly, A.K. (1979) Thermoluminescence of quartz. Part iv: effects of stress on sensitivity. *Indian Journal Pure and Applied Physics* **17**, 655–657.

Falguères, C., Miallier, D., Sanzelle, S., Faïn, J., Laurent, M., Montret, M., Pilleyre, Th. and Bahain, J.J. (1994) Potential use of the E' center as an indicator of initial resetting in TL/ESR dating volcanic materials. *Quaternary Science Reviews* **13**, 619–623.

Kieffer, S.W. (1971) Shock metamorphism of the Coconino sandstone at Meteor Crater, Arizona. *Journal of Geophysical Research* **76**, 5449–5473.

Miallier, D., Faïn, J., Montret, M., Pilleyre, Th., Sanzelle, S. and Soumana, S. (1991) Properties of the red TL peak of quartz relevant to thermoluminescence dating. *Nuclear Tracks and Radiation Measurements* **18**, 89–94.

Montret, M. (1980) Distribution spatiale de l'énergie déposée par des ions énergétiques dans les milieux condensés. Etude par thermoluminescence. Thesis, Univ. Clermont II, Clermont-Ferrand, France.

Pilleyre, Th. (1991) Datation par thermoluminescence. Application à la chronologie des retombées volcaniques. Thesis, Univ. Blaise Pascal, Clermont-Ferrand, France.

Pilleyre, Th., Montret, M., Faïn, J., Miallier, D. and Sanzelle, S. (1992) Attempts at dating ancient volcanoes using the red TL of quartz. *Quaternary Science Reviews* **11**, 13–17.

Prescott, J.R. and Hutton, J.T. (1988) Cosmic and gamma ray dosimetry for TL and ESR. *Nuclear Tracks and Radiation Measurements* **14**, 223–227.

Prescott, J.R. and Hutton, J.T. (1994) Cosmic-ray contributions to dose rates for luminescence and ESR dating: large depths and long-term time variations. *Radiation Measurements* **23**, 497–500.

Prescott, J.R. and Stephan, L.G. (1982) The contribution of cosmic radiation to the environmental dose for thermoluminescence dating. *PACT Journal* **6**, 17–25.

Sutton, S.R. (1985) Thermoluminescence measurements on shock-metamorphosed sandstone and dolomite from meteorite crater, Arizona. 1. Shock dependence of thermoluminescence properties. *Journal of Geophysical Research* **90**(B5), 3683–3689.

Sutton, S.R. (1985) Thermoluminescence measurements on shock-metamorphosed sandstone and dolomite from meteor crater, Arizona. 2. Thermoluminescence age of meteor crater. *Journal of Geophysical Research* **90**(B5), 3690–3700.

Vincent, P.M., Beauvillain, A., Boudeule, M. and Moutaye, A.H. (1994) The astrobleme of Aorounga (Sahara of Tchad): preliminary structural data. *Impact-cratering third international workshop*, Limoges-Rochechouart, France (Abstract).